Structure−Property Relationships of Halogen-Free Flame-Retarded Poly(butylene terephthalate) and Glass Fiber Reinforced PBT

T. Köppl,[1] S. Brehme,[2] F. Wolff-Fabris,[1] V. Altstädt,[1] B. Schartel,[2] M. Döring[3]

[1]*University of Bayreuth, Department Polymer Engineering, Universitätsstr. 30, 95447 Bayreuth, Germany*
[2]*BAM Federal Institute for Materials Research and Testing, Unter den Eichen 87, 12205 Berlin, Germany*
[3]*Karlsruhe Institute of Technology, Institute of Technical Chemistry, 76021 Karlsruhe, Germany*

Received 26 January 2011; accepted 15 May 2011
DOI 10.1002/app.34910
Published online 30 September 2011 in Wiley Online Library (wileyonlinelibrary.com).

ABSTRACT: Flame retardancy for thermoplastics is a challenging task where chemists and engineers work together to find solutions to improve the burning behavior without strongly influencing other key properties of the material. In this work, the halogen-free additives aluminum diethylphosphinate (AlPi-Et) and a mixture of aluminum phosphinate (AlPi) and resorcinol-bis(di-2,6-xylyl phosphate) (AlPi-H + RXP) are employed in neat and reinforced poly(butylene terephthalate) (PBT), and the morphology, mechanical performance, rheological behavior, and flammability of these materials are compared. Both additives show submicron dimensions but differ in terms of particle and agglomerate sizes und shapes. The overall mechanical performance of the PBT flame-retarded with AlPi-Et is lower than that with AlPi-H-RXP, due to the presence of larger agglomerates. Moreover, the flow behavior of the AlPi-Et/PBT materials is dramatically changed as the larger rod-like primary particles build a percolation threshold. In terms of flammability, both additives perform similar in the UL 94 test and under forced-flaming combustion. Nevertheless, AlPi-Et performs better than AlPi-H + RXP in the LOI test. The concentration required to achieve acceptable flame retardancy ranges above 15 wt %. © 2011 Wiley Periodicals, Inc. J Appl Polym Sci 124: 9–18, 2012

Key words: polyesters; fibers; morphology; structure–property relations; flame retardance

INTRODUCTION

Poly(butylene terephthalate) (PBT) is a technical thermoplastic used as neat or as fiber reinforced material for applications in electrical and electronic devices, communication, and automotive parts, due to its outstanding mechanical properties. In all these applications, the burning behavior of the material plays a decisive role, and this is unfortunately one of the disadvantages of this polymer. The incorporation of flame-retardants is therefore required and may render this highly flammable thermoplastic suitable for the above-mentioned applications. However, the incorporation of such additives should not lead to a too dramatic negative effect on the mechanical stability and processability of the polymer. Furthermore, when considering reinforced PBT (i.e., glass fibers), a further challenge arises. Typically, the incorporation of glass fibers in PBT has a major impact on the burning behavior, leading to a higher flammability as less material is removed by melt flow or dripping during the fire and less heat is discharged from the pyrolysis zone. Generally, this results in the need of employing larger flame-retardant contents to meet requirements.

Typical flame-retardant additives for thermoplastics includes: halogenated systems based on bromine and chlorine, organic, or inorganic compounds containing phosphorus, inorganic metal hydroxides, boron, and nitrogen compounds and combinations thereof, which lead to synergistic effects and mechanisms.[1]

The most effective additives nowadays are halogen-containing substances, acting particularly on the gas phase, and the required amount is relative low compared to other additives. However, halogen-containing additives have to be replaced due to European Union regulations for protection of environment and health.[2] The first approaches regarding halogen-free additives are already commercially available. Nevertheless, due to the lower flame protection performance, in comparison to halogen-containing additives, significantly higher additive contents have to be employed, having primarily a dramatic negative influence on the mechanical performance. The most relevant halogen-free additives for thermoplastic polyesters like PET and PBT are based on nitrogen,

Correspondence to: T. Köppl (thomas.koeppl@uni-bayreuth.de).

Contract grant sponsor: German Research Foundation (DFG); contract grant number: AL 474/17-1

mainly melamine derivatives, metal hydroxides like aluminum and magnesium hydroxide and phosphorus-containing substances like organic and inorganic phosphates, phosphonates, and phosphinates as well as red phosphorus.[3,4]

In this work, aluminum phosphonates (AlPi) are used as flame-retardants for PBT, which are one of the few commercially available halogen-free flame retardants specially designed for PBT. In the literature, the positive effect of such metal phosphinates like aluminum and zinc phosphinates in terms of flame retardancy has already been successfully reported.[5–8] Quite surprisingly, although, other material's key properties of these modified polyesters were not investigated. There is therefore a lack in the literature regarding the overall effect of such halogen-free additives on the processability, morphology, and particularly mechanical behavior of the polymer, as typical studies concentrated exclusively on the burning behavior.

This study particularly fills this gap, presenting the overall structure–properties relationships of neat and glass fiber reinforced flame-retarded PBT in terms of the mechanical performance, rheological behavior, and flammability. Quite importantly, these results are correlated to the morphology of the halogen-free additive particles, providing significant hints for the further development of new flame retardants, which besides an outstanding flame retardancy should also only play a marginal influence on other polymer properties.

EXPERIMENTAL WORK

Materials and processing

An injection-molding grade of PBT (Ultradur B4520, BASF SE, $T_M = 223°C$) is used. In this work, two additives based on AlPi are compared: Exolit OP 1240 containing aluminum diethylphosphinate (AlPi-Et) from Clariant with a phosphor content of 24 wt % and Phoslite B85AX containing 85 wt % AlPi and 15 wt % resorcinol-bis(di-2,6-xylyl phosphate) (AlPi-H + RXP) from Italmatch Chemicals with a phosphor content of 36 wt %. These materials are melt compounded using a Werner and Pfleiderer Megacompounder ZSK 26 MCC corotating twin-screw extruder with a length-to-diameter ratio of 44 at a maximum temperature of 250°C. The flame-retardants are supplied in the main feeder together with the dried polymer.

Compounds with a flame-retardant concentration based on the recommended content from additive producer (20 wt % additive), as well as compounds with a phosphor-content of 1.5 wt % are produced to compare the material on the same flame-retardancy level (6.3 wt % of AlPi-Et and 4.2 wt % of AlPi-H + RXP, respectively).

Reinforced PBT is produced by adding 30 wt % glass fibers from PPG (fiber Glass ChopVantage HP 3786) with a diameter of 10 μm and an initial length of 4.5 mm. The fibers are fed near the die with a corotating side feed.

The compounded material is dried for 4 hours at 100°C before testing specimens are produced by injection molding. The neat and reinforced samples are produced on an Arburg Allrounder 320 S 500-150 with a melt temperature of 250°C and a mold temperature of 70°C. The rheological samples are pressed in a hot press under vacuum for 5 minutes under a pressure of 20 kN at 250°C. All samples are dried at 80°C in a vacuum dryer for at least 24 hours before the characterization to avoid moisture effects.

Characterization

Morphology

The morphology of the materials is characterized by scanning (SEM) and transmission (TEM) electron microscopy as well as by microcomputertomography (μ-CT). The micrographs are obtained with a SEM from Jeol JSM-IC 848 with an acceleration voltage of 15 kV and a TEM from Zeiss type 902 with an acceleration voltage of 80 kV. For TEM, ultrathin samples are cut using a microtome Ultracut E from Leica. The SEM-pictures are taken from fracture surfaces after impact tests.

To analyze the particle size and distribution, μ-CT measurements are performed. The measurements are run on a Skyscan 1072-100 kV with a cylindrical specimen of 4 mm height and 4 mm diameter. The X-ray source has a voltage of 80 kV and a current of 90 μA with a magnification of 50×, which match a resolution of 5 μm per pixel. The 360° X-ray projections are reconstructed and afterwards evaluated by MAVI-Software from FhG ITWM Kaiserslautern. By means of this three-dimensional analysis, with a resolution of 5 μm/pixel, it is possible to identify particles larger than 20 μm.

Crystallinity analysis

Differential scanning calorimetry (DSC) investigations are carried out with a Mettler Toledo DSC/SDTA 821e. The crystallinity is analyzed under N_2-atmosphere with a cooling rate of 10 K/min and an enthalpy of fusion of a 100% crystalline PBT of 140 J/g.[9]

Rheological behavior

Rheological properties are investigated by a stress controlled dynamic-mechanical rheometer SR 5000 from Rheometric Scientific with plate-plate geometry

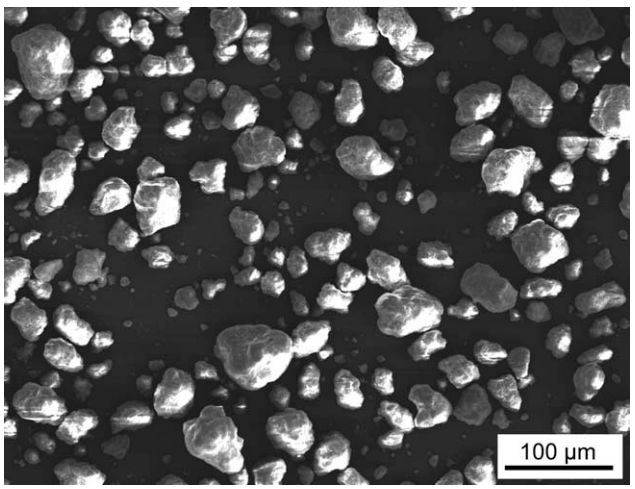

Figure 1 Structure of AlPi-Et (SEM micrograph).

under nitrogen atmosphere. The pressed samples have diameter of 25 mm and height of 2 mm and are analyzed isothermally at 240°C. Dynamic-mechanical tests are performed to compare the complex viscosity of the materials in dependence of the angular frequency. Each measurement is repeated at least four times.

Flammability tests

The flammability (reaction to a small flame) of the materials is assessed by UL 94 test according to IEC 60695-11-10 and by limiting oxygen index (LOI) according to ISO 4589. The fire behavior under forced-flaming combustion is investigated using a cone calorimeter (Fire Testing Technology, East Grinstead, UK) according to ISO 5660. Plate-shaped specimen ($100 \times 100 \times 3$ mm^3) are placed in aluminum trays and exposed to an irradiation of 50 kW m^{-2}. Every material is tested at least twice.

Mechanical testing

Tensile and Charpy impact tests are performed to analyze the mechanical behavior of the composites at room temperature. The tensile tests are carried out on a universal testing machine Zwick Z020 according to ISO 527 with a crosshead speed of 5 mm/min. The specimens were prepared according to ISO 3167 (Type A). Impact properties were evaluated by the unnotched Charpy test (ISO 179 fU) using a Zwick/Roell RKP 5113 with a pendulum energy of 50 J.

RESULTS AND DISCUSSION

Properties of neat PBT

Morphology

First, the particle morphology of the halogen-free additives is investigated with SEM. AlPi-Et consists of agglomerates with a size from 10 to 100 µm (Fig. 1) and AlPi-H + RXP shows smaller agglomerates with a size of 5–50 µm (Fig. 2). Subsequently, the size and dispersion of the particles in the polymer matrix after melt compounding were analyzed by TEM and µ-CT. TEM allows the analysis of the shape and size of particles in nanometer scale. Figures 3 and 4 show the polymer containing 6.3 wt % AlPi-Et and 4.2 wt % AlPi-H + RXP, respectively. These flame-retardant contents correspond to a total phosphorus amount of 1.5 wt %. The particles are partially or completely segregated from the primary agglomerates by the compounding step in both systems. Therefore, both systems have a similar nanocomposite-like morphology. The size distribution of the particles and small agglomerates in nanometer scale can be observed in Figure 5. The AlPi-Et particles and agglomerates have a length-range from 50 nm to 2 µm with a median length of 240 nm.

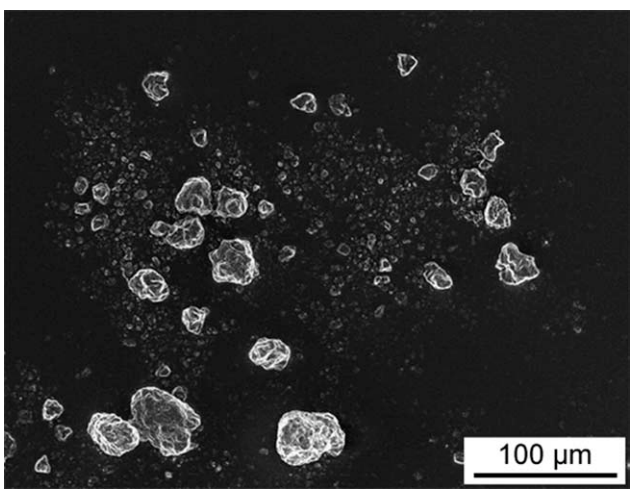

Figure 2 Structure of AlPi-H + RXP (SEM micrograph).

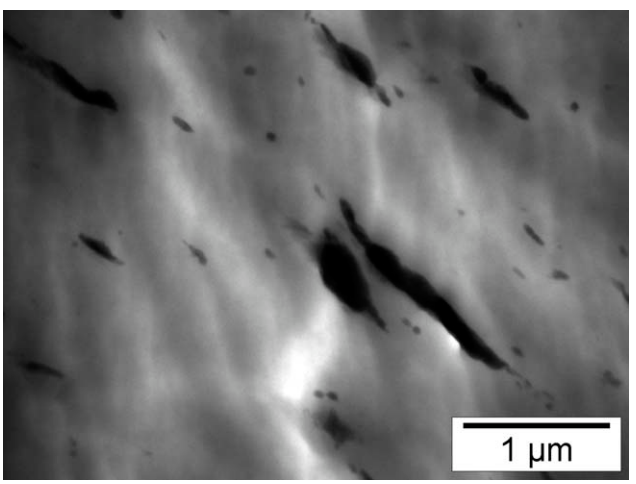

Figure 3 TEM image of PBT + AlPi-Et 6.3.

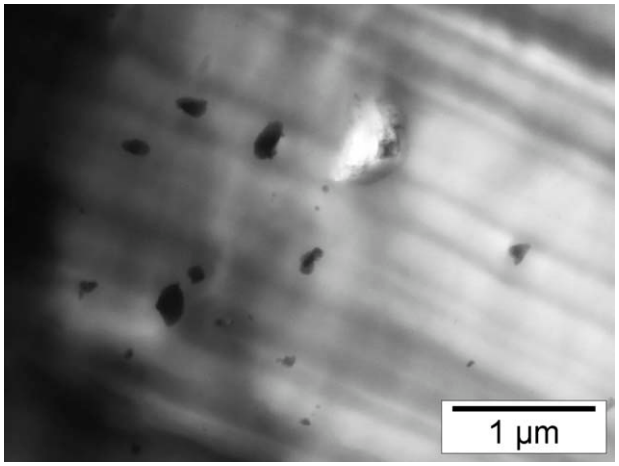

Figure 4 TEM image of PBT + AlPi-H + RXP 4.2.

These rod-like primary particles can be seen in Figure 3. The AlPi-H + RXP domains show diameters between 50 and 350 nm with a significantly lower median length of 110 nm. In contrast to AlPi-Et, the particles show primarily a spherical shape (Fig. 4).

As previously mentioned, after compounding, some particle agglomerates were still present in the polymer matrix, and their size was further analyzed by µ-CT, which allows detecting the agglomerates in micrometer scale down to a dimension of 20 µm. As example, a three dimensional reconstruction of the 360° X-ray projections of the polymer containing 6.3 wt % AlPi-Et can be seen in Figure 6. The size distribution of the agglomerates for both flame-retardants is found at the same range and can be seen in Figure 7. The results show that the agglomerates of the AlPi-Et flame retardant have a slightly higher median length (around 35 µm) than the AlPi-H + RXP agglomerates (around 30 µm). When increasing the flame-retardant concentration to 20 wt % we observe the same agglomerate size as for the lower concentrations but consequently a higher total number of agglomerates.

These results regarding the morphology of the flame retardant particles as well as the morphology of the flame-retarded polymer are of major importance for the identification of structure–property relationships and are correlated to the overall properties of the neat and glass fiber reinforced PBT in the next sections of this study.

Rheological properties

Dynamic mechanical tests in dependence of angular frequency were performed to investigate the flow characteristics of the polymer melt, which are related to the polymer processability, for instance in injection molding applications. These investigations were carried out at a temperature of 240°C, as the polymer is totally fused. The absolute value of the complex viscosity $|\eta^*|$ is compared at different filler amounts of the flame-retardants. Pure PBT shows within the applied frequency range from 0.6 to 100 rad/s no significant change of $|\eta^*|$ and has therefore a Newtonian behavior at $\sim$ 400 Pa s (Fig. 8).

By addition of the flame-retardant additives, a higher viscosity especially at low frequencies is expected because the solid particles are not deformable and more stress is necessary to attain the same melt deformation. However, the addition of AlPi-Et in the amount of 6.3 wt % leads to no increase of $|\eta^*|$. This composite shows nearly the same flow

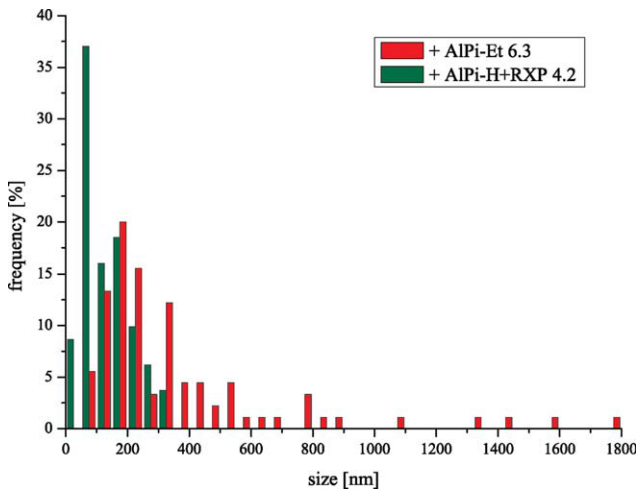

Figure 5 Primary particle distribution of PBT + AlPi-Et or AlPi-H + RXP (1.5% *P*) obtained by evaluation of TEM images. [Color figure can be viewed in the online issue, which is available at wileyonlinelibrary.com.]

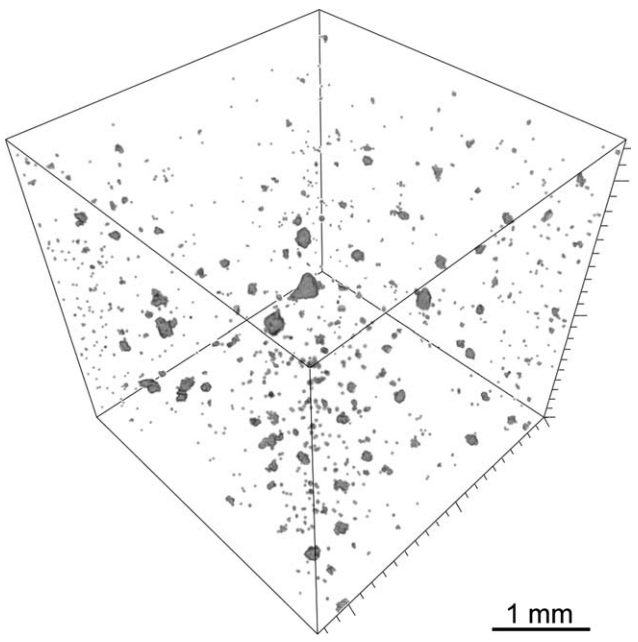

Figure 6 Three-dimensional reconstruction of PBT + AlPi-Et 6.3 (µ-computer-tomography).

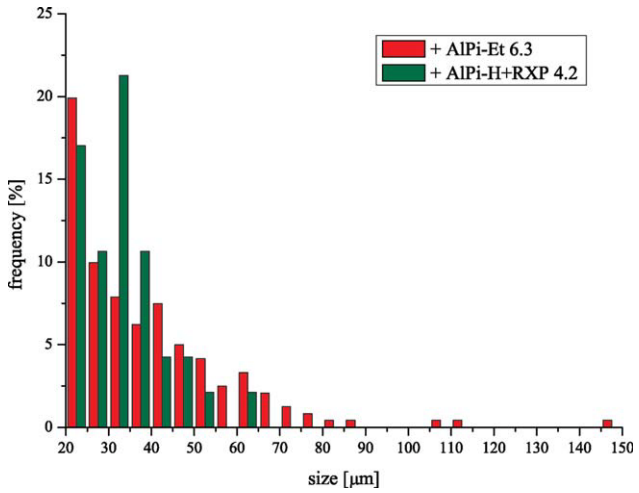

Figure 7 Particle agglomerate distribution of PBT + AlPi-Et or AlPi-H + RXP (1.5% *P*) obtained by evaluation of µ-computer-tomography. [Color figure can be viewed in the online issue, which is available at wileyonlinelibrary.com.]

behavior as pure PBT. However, the addition of 20 wt % AlPi-Et leads to a significant increase of the viscosity at frequencies under 10 rad/s. This rapid increase of viscosity with decreasing frequency is in the literature described as flow limit.[10] This result shows that the concentration of 20 wt % is above the rheological percolation threshold of the system, leading to the formation of a network. In this case, the solid particles have contact to each other and hinder the deformation of the polymer chains. At higher frequencies above 20 rad/s the viscosity is in the same range as pure PBT. The stress is high enough to overcome the percolation as the formed network is destroyed, and consequently, the molten chains are free to move.

The same characterization was performed with the AlPi-H + RXP composites, and the viscosity behavior can be seen in Figure 9. There is a small increase of viscosity at both AlPi-H + RXP concentrations to around 500 Pa s in the whole frequency range. This Newtonian behavior is observed even at a concentration of 20 wt % AlPi-H + RXP, showing that in this case, no flow limit and percolation network can be observed. The reason for this distinct behavior, in comparison to AlPi-Et, is related to the morphology of the additive particles. The AlPi-Et primary particles are at least twice larger in median size than the AlPi-H + RXP particles and have a much higher aspect ratio. Owing to their rod-like shape the particles come earlier into contact to each other, which results also in an earlier formation of a percolation network in comparison to the spherical particles of AlPi-H + RXP.

Flammability

PBT is quite flammable as shown by the low LOI value of 23.3% and a HB classification in UL 94 (Table I). The addition of 6.3 wt % AlPi-Et led to an increase in LOI (27.5%) and a better UL 94 result (V-2). Furthermore, by adding 20 wt % AlPi-Et the LOI was strongly increased and the best classification in UL 94 (V-0) was reached. Flaming drips were prevented due to the presence of a flow limit. Large increases in LOI when adding AlPi-Et to PBT have been previously reported and attributed to effective flame inhibition.[5,11–13] This means that 20 wt % AlPi-Et leads to an excellent flame retardancy of PBT.

The addition of 4.2 wt % AlPi-H + RXP did not result in any increase of LOI. Nevertheless, the

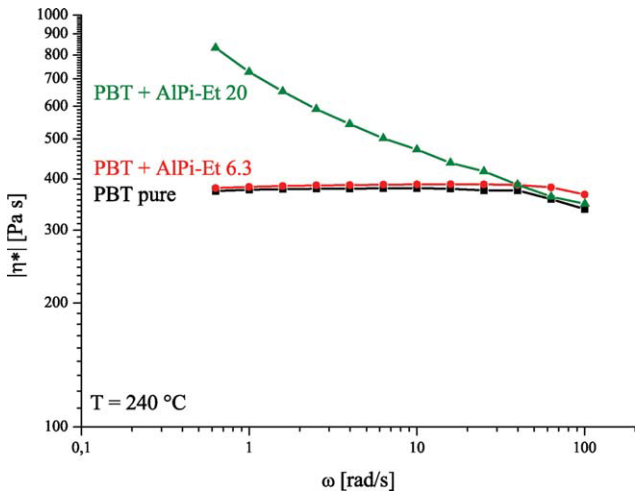

Figure 8 AlPi-Et composites: Complex shear viscosity in dependence of angular frequency. [Color figure can be viewed in the online issue, which is available at wileyonlinelibrary.com.]

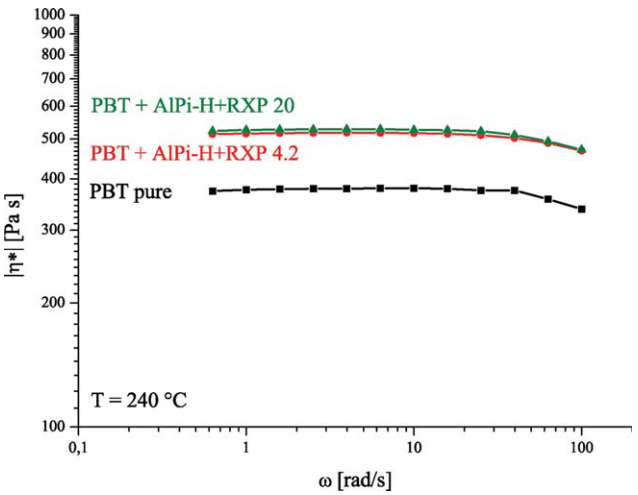

Figure 9 AlPi-H + RXP composites: Complex shear viscosity in dependence of angular frequency. [Color figure can be viewed in the online issue, which is available at wileyonlinelibrary.com.]

TABLE I
Flammability (Reaction to a Small Flame) of the Neat PBT Formulations in LOI (Error ± 1%) and UL 94 as well as Results Obtained by Cone Calorimetry with an External Heat Flux of 50 kW/m²

Material	*P*-content (wt %)	LOI (%)	UL 94	pHRR (kW/m²)	THE (MJ/m²)	Residue (wt %)	THE/TML (MJ/m²g)
PBT	0	23.3	HB	1812 ± 100	76 ± 2	4 ± 1	2.1 ± 0.1
+ AlPi-Et 6.3	1.5	27.5	V-2	1412 ± 100	60 ± 1	5 ± 1	1.7 ± 0.1
+ AlPi-Et 20	4.8	52.0	V-0	657 ± 70	45 ± 1	11 ± 1	1.3 ± 0.1
+ AlPi-H + RXP 4.2	1.5	23.2	V-2	1188 ± 100	66 ± 1	7 ± 1	1.9 ± 0.1
+ AlPi-H + RXP 20	7.1	26.8	V-2	400 ± 40	41 ± 1	20 ± 1	1.3 ± 0.1

pHRR, Peak of heat release rate; THE, Total heat evolved; TML, Total mass loss.
Errors based on maximum deviation of average values.

UL 94 classification was improved to V-2. Increasing the amount of AlPi-H + RXP to 20 wt % led to an improved LOI. The UL 94 result remained V-2 because there was no flow limit to prevent flaming drips. Therefore, the flame retardancy of PBT with AlPi-H + RXP did not yield satisfying results with respect to the LOI and UL 94.

Under forced-flaming conditions, both flame-retardants decreased the peak heat release rate (pHRR) and the total heat evolved (THE) compared to PBT (Table I). Concerning the reduction of the pHRR, AlPi-H + RXP was more effective than AlPi-Et with respect to the same phosphorus content as well as referring to the same additive content. Considering the reduction in THE, AlPi-Et performed better than AlPi-H + RXP in terms of the same phosphorus content. Otherwise, regarding the same additive content, there was a slight advantage for AlPi-H + RXP. The increase in residue proves that both flame-retardants exhibit a condensed-phase activity, which is strong for AlPi-H + RXP and moderate for AlPi-Et. Further, the effective heat of combustion, THE/TML (TML = total mass loss), was clearly decreased due to flame inhibition. Thus, both flame-retardants exhibited a strong gas-phase mechanism. The flame inhibition was equally strong for both flame-retardants because there were no significant differences in the reduction of THE/TML.

The flame-retarded PBT materials with the two additives were compared referring to the same phosphorus content of the material (i.e., 1.5 wt % P) and the same additive content (i.e., 20 wt %). Concerning the same phosphorus content, both flame-retardants exhibited a similar performance under forced-flaming conditions as well as concerning the reaction to a small flame (LOI, UL 94). Referring to the same additive content, AlPi-H + RXP performed better under forced-flaming conditions than AlPi-Et, whereas AlPi-Et led to better results under the very specific conditions of LOI and UL 94, respectively.

Mechanical properties

The influence of the flame-retardant additives on the mechanical properties is evaluated on quasi-static (tensile) and dynamic (impact) testing. The results of the pure as well as the flame-retarded PBT are summarized in Table II. In this table, the following properties are presented: Young's modulus (E) for evaluation of the stiffness, the maximal tensile strength σ_m for strength, the unnotched impact strength a_{cu} for toughness and the elongation at break ε_b for ductility.

The size and shape of the particles, the adhesion to the matrix, and the dispersion of the particles play a decisive role on the mechanical properties of these filled polymers.

First, however, the influence of the particles on the polymer crystallinity has to be investigated. Typically, a higher crystallinity leads to higher stiffness and lower toughness. In the case of this study, the neat PBT shows a crystallinity of around 34%. This value is slightly reduced to ~ 31% when incorporating 20 wt % of the flame retardants (Table II). Although a change of crystallinity should definitely affect the mechanical properties, the minimal reduction of crystallinity observed in this study (from 34 to 31%) is expected to play only a negligible role on

TABLE II
Mechanical Properties of Neat PBT with AlPi-Et or AlPi-H + RXP

Material	Crystallinity (%)	E [MPa]	σ_m (MPa)	ε_b (%)	a_{cu} (kJ/m²)
PBT	34 ± 1	2170 ± 30	54 ± 1	21 ± 1	190 ± 4
+ AlPi-Et 6.3	34 ± 1	2630 ± 70	47 ± 1	8 ± 1	30 ± 8
+ AlPi-Et 20	31 ± 1	2800 ± 20	35 ± 1	5 ± 1	20 ± 1
+ AlPi-H + RXP 4.2	35 ± 2	2450 ± 50	54 ± 1	21 ± 2	89 ± 4
+ AlPi-H + RXP 20	31 ± 2	2400 ± 100	46 ± 1	19 ± 3	58 ± 2

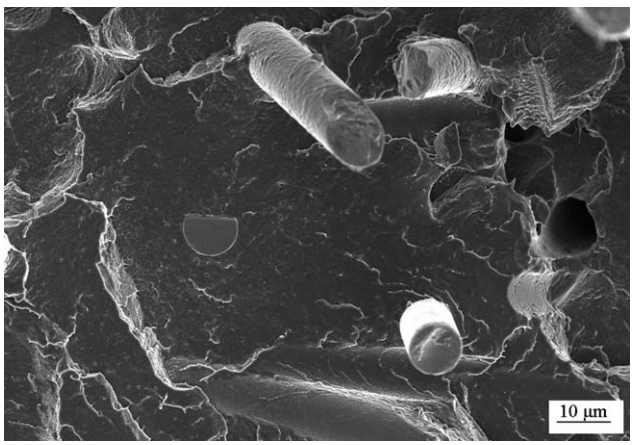

Figure 10 SEM image of the fracture surface of PBT GF 30.

the overall mechanical properties, and the incorporation of additives is the main factor responsible for the dramatic changes observed on the mechanical behavior.

By adding solid additives, an increase of Young's modulus in dependence of the filler amount is expected, as the solid particles have a higher stiffness than the polymer. This is also observed in this work, as the modulus increases around 10% for the lower amounts of flame-retardants and up to 30% at the loading of 20 wt %. Therefore, the stiffness of PBT is increased by both flame-retardants. This increase is higher for the AlPi-Et additive due to the higher aspect ratio of the rod-like particles in comparison to the spherical AlPi-H + RXP particles.

The addition of 6.3 wt % AlPi-Et leads also to a significant decrease of tensile strength (15%) in comparison to the addition of 4.2 wt % AlPi-H + RXP. Furthermore, filler content of 20 wt % results in a decrease of strength and elongation in both systems but particularly pronounced in the AlPi-Et composites. A similarly stronger influence of AlPi-Et is pointed out by the impact test. The different behavior of the two composite systems can be explained with the particle agglomerate size. As described in literature,[14] the strength decreases with increasing particle size. As the additive AlPi-H + RXP has smaller particles and agglomerates, a less negative influence on strength and toughness than AlPi-Et can be seen, suggesting also that the cohesive forces of the agglomerates are relatively low.

Properties of reinforced PBT

Morphology

The glass fibers themselves as well as the fracture surfaces of the reinforced samples after impact testing were investigated by SEM. The fibers show a diameter as declared of 10 ± 1 µm and an unknown proprietary sizing on the surface.

Regarding the reinforced polymers, in all three composite systems (without additive, with AlPi-Et and with AlPi-H + RXP) a good dispersion of the fibers in the PBT matrix is obtained.

The reinforced PBT without additive and the composites with AlPi-H + RXP show a relative poor fiber-matrix adhesion (Figs. 10 and 11, respectively). Quite interestingly, the fiber-matrix adhesion of the AlPi-Et composites seems to be stronger, as the fibers are partly covered by the matrix (Fig. 12).

Flammability

The reinforcement of PBT with glass fibers increases its flammability although combustible polymer is replaced by inert glass. This is because the glass fibers suppress the melt flow and dripping typically observed for PBT. Thus, heat is no longer taken away from the pyrolysis zone by melt flow or dripping. Furthermore, a "wick-effect" of the glass fibers or the improvement of the heat transmission to the part of the material below the burning region was

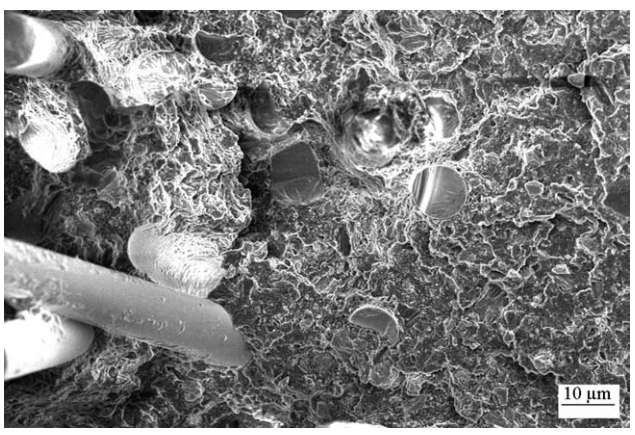

Figure 11 SEM image of the fracture surface of PBT GF 30 + AlPi-H + RXP 20.

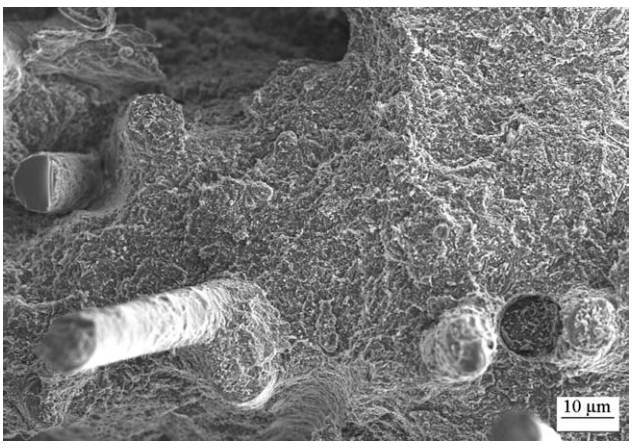

Figure 12 SEM image of the fracture surface of PBT GF 30 + AlPi-Et 20.

TABLE III
Flammability (Reaction to a Small Flame) of the Reinforced PBT Formulations in LOI (Error ± 1%) and UL 94 as well as Results Obtained by Cone Calorimetry with an External Heat Flux of 50 kW/m^2

Material	*P*-content (wt %)	LOI (%)	UL 94	pHRR (kW/m^2)	THE (MJ/m^2)	Residue (wt %)	THE/TML (MJ/m^2 g)
PBT GF 30	0	19.8	HB	677 ± 40	59 ± 1	30 ± 1	1.9 ± 0.1
+ AlPi-Et 4.4	1	33.9	HB	438 ± 40	41 ± 2	33 ± 1	1.4 ± 0.1
+ AlPi-Et 6.3	1.5	39.0	HB	367 ± 30	39 ± 1	31 ± 1	1.3 ± 0.1
+ AlPi-Et 14	3.3	43.3	V-0	351 ± 30	37 ± 1	37 ± 1	1.3 ± 0.1
+ AlPi-Et 20	4.8	36.7	V-0	310 ± 30	40 ± 1	40 ± 1	1.5 ± 0.1
+ AlPi-H + RXP 4.2	1.5	21.7	HB	378 ± 30	44 ± 2	34 ± 1	1.5 ± 0.1
+ AlPi-H + RXP 20	7.1	31.9	V-0	165 ± 15	35 ± 2	55 ± 1	1.7 ± 0.1

pHRR, Peak of heat release rate; THE, total heat evolved; TML, total mass loss.
Errors based on maximum deviation of average values.

proposed as possible reason in the literature.[15] As consequence, the LOI value of 19.8% for the glass fiber reinforced PBT is lower than for neat PBT (23.3%).

Adding 4.2 wt % AlPi-H + RXP to glass fiber reinforced PBT increased the LOI slightly to 21.7% (Table III). The UL 94 classification remained HB. The addition of 20 wt % AlPi-H + RXP resulted in a significant increase in LOI and improved the UL 94 classification to V-0. Thus, good flame retardancy is achieved for reinforced PBT with 20 wt % AlPi-H + RXP. Using 4.4 wt % or 6.3 wt % AlPi-Et, the LOI was strongly increased to 33.9 and 39.0%, respectively, while the UL 94 rating remained HB. Adding 14 wt % AlPi-Et the LOI was increased further to 43.3% and UL 94 was improved to a V-0 classification. The material is well flame-retarded at this point. Interestingly, the LOI decreased again when higher amounts of AlPi-Et (i.e., 20 wt %) were used (Fig. 13). Thus, the flame retardancy was decreased if too much AlPi-Et has been added. Such behavior has also been reported for red phosphorus in nylon 6 and ascribed to the inherent flammability of red phosphorus.[16] In conclusion, there is an optimum concentration of AlPi-Et in glass fiber reinforced PBT of about 13 wt %. At this point, it has to be noted that the additive content as well as the phosphorus content is given with respect to the whole material, that is, including glass fibers. Referring to the PBT fraction only, the phosphorus content is correspondingly higher.

Under forced-flaming conditions, both flame-retardants decreased the pHRR and the THE with respect to neat PBT due to gas-phase and condensed-phase activity. With respect to the same phosphorus content, there was no significant difference in the reduction of the pHRR while the THE was reduced a slightly more by AlPi-Et than by AlPi-H + RXP. Referring to the same additive content, AlPi-H + RXP reduced pHRR and THE more than AlPi-Et. The gas-phase activity was equally strong for the two flame-retardants whereas the condensed-phase activity was moderate for AlPi-Et and strong for AlPi-H + RXP. Analogous to LOI, the THE indicated that there is an optimum concentration of AlPi-Et in glass fiber reinforced PBT. The THE was lowest for 14 wt % of AlPi-Et and increased if higher amounts were added.

AlPi-Et performed better than AlPi-H + RXP as a flame retardant for glass fiber reinforce PBT under the very specific conditions of LOI. The performance of both flame-retardants in the UL 94 was similar. Under forced-flaming conditions, AlPi-Et was slightly better than AlPi-H + RXP based on the same phosphorus content whereas AlPi-H + RXP performed clearly better based on the same additive content.

Mechanical properties

As expected the incorporation of glass fiber reinforcement into PBT leads to a distinct increase of modulus (four times) and tensile strength (two times), and a reduction of elongation at break (80%

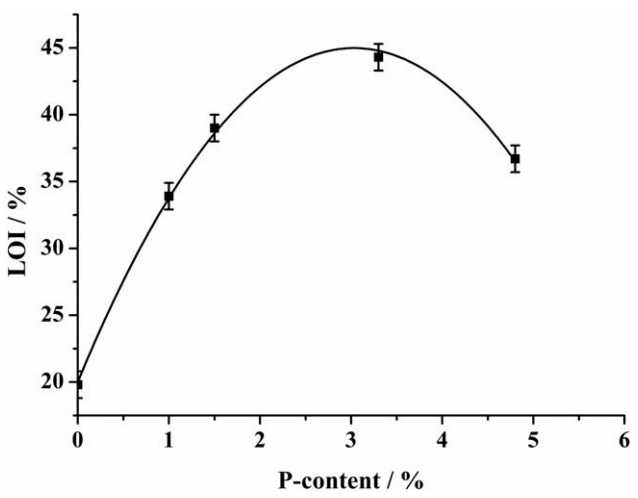

Figure 13 Dependence of LOI on the phosphorus content of glass fiber reinforced PBT flame retarded with AlPi-Et.

TABLE IV
Mechanical Properties of Reinforced PBT with AlPi-Et or AlPi-H + RXP

Material	E (MPa)	σ_m (MPa)	ε_b (%)	a_{cu} (kJ/m^2)
PBT GF 30	8090 ± 130	124 ± 2	4 ± 1	65 ± 3
+ AlPi-Et 4.4	8130 ± 340	119 ± 1	4 ± 1	59 ± 3
+ AlPi-Et 6.3	8740 ± 150	119 ± 1	4 ± 1	61 ± 3
+ AlPi-Et 14	8750 ± 220	99 ± 2	2 ± 1	45 ± 3
+ AlPi-Et 20	10,290 ± 300	93 ± 1	2 ± 1	27 ± 2
+ AlPi-H + RXP 4.2	8120 ± 260	116 ± 1	3 ± 1	47 ± 3
+ AlPi-H + RXP 20	9200 ± 400	99 ± 2	2 ± 1	39 ± 3

decline) and impact strength (65% decline) (Table IV). The values for PBT GF 30 are comparable to literature data.[17] By adding the flame retardant particles the modulus increases with the concentration while the tensile strength as well as the elongation and impact strength decrease. This is in accordance with the results related to the unreinforced PBT. When comparing both 20 wt % flame retardant systems, the addition of AlPi-Et leads to a lower tensile and impact strength. The reason is the previously discussed lower surface area of the particles in comparison to the AlPi-H + RXP composites, as seen on the unreinforced polymer. In contrast, the modulus of the AlPi-Et compounds is around 10% higher due to a better fiber-matrix adhesion than in the AlPi-H + RXP compounds.

CONCLUSIONS

In this study, the AlPi flame-retardant additives AlPi-Et and AlPi-H + RXP were incorporated in neat and glass fiber reinforced PBT. These additives are available under the form of agglomerates (in the range of the micrometer scale) of single particles (in the range of the nanometer scale). In all cases, a satisfactory dispersion of the additives was obtained by melt compounding, Even though some particle agglomerates could still be observed, dispersed single particles were also present.

The different particle size and shape of these additives (rod-like particles for AlPi-Et and sphere-like particles for AlPi-H + RXP) had major influence on mechanical and rheological properties of the modified PBT. Regarding the mechanical properties, the use of these solid additives led to an increase of the Young's modulus of the modified polymer. However, the tensile and impact strength were significantly reduced. This reduction was less pronounced for the polymer modified with AlPi-H + RXP, due to the presence of smaller agglomerates, in comparison to AlPi-Et. Moreover, the shape of the particles also played an additional role in terms of the rheological behavior. Hence, already 20 wt % of rod-like AlPi-Et particles led to a flow limit and a rheological percolation threshold, in contrast to the spherical particles of AlPi-H + RXP, with which the percolation was not reached within the amounts of additive used in this study. Moreover, a concentration of 20 wt % of either of the additives was observed to be sufficient to attain suitable fire retardancy for unreinforced PBT as assessed by UL 94 and cone calorimetry. Concerning LOI, AlPi-Et performed better than AlPi-H + RXP.

Regarding the fiber reinforced composites, the matrix AlPi-Et/PBT showed a much better fiber-matrix adhesion than in the case AlPi-H + RXP/PBT, consequently resulting in higher Young's modulus. The glass fiber reinforced PBT composites were successfully flame-retarded with either of the additives, with AlPi-Et showing better performance only in terms of LOI.

In summary, it could be observed that the amount of AlPi-based additives required for suitable flame retardancy, in both unreinforced and reinforced PBT, leads to a significant reduction of the stress and strain at break of the polymer. Therefore, a compromise among flammability, processability, and overall mechanical properties has to be met, depending on the desired application.

PBT was kindly provided by BASF SE, Ludwigshafen, and the flame-retardant additives by Clariant Additives, Sulzbach, and Walter Thieme Handel GmbH, Stade. The authors further acknowledge Anne Lang and Carmen Kunert (Department of Polymer Engineering) for the experimental support in the field of microscopy.

References

1. Levchik, S.V.; Weil, E. D. Polym Int 2005, 54, 11.
2. EU-Council and Parliament, RoHS–Directive, 2002/95/EC, 2003.
3. Leisewitz, A.; Kruse, H.; Schramm, E. Umweltbundesamt, Report 40/01, 2001.
4. Weil, E. D.; Levchik, S. V. J Fire Sci 2004, 22, 339.
5. Braun, U.; Bahr, H.; Sturm, H.; Schartel, B. Polym Adv Technol 2008, 19, 680.
6. Jenewein, E.; Kleiner, H.-J.; Wanzke, W.; Budzinsky, W. International Patent WO 97/39053, 1997.
7. Kleiner, H.-J.; Budzinsky, W. Int. Pat. WO 9839381 (1998).
8. Costanzi, S.; Leonardi, M. Int. Pat. WO 2005121232 (2005).
9. Wunderlich, B. Thermal analysis of polymeric materials; Springer: Berlin, 2005.

10. Cassagnau, P. Polymer 2008, 49, 2183.
11. Gallo, E.; Braun, U.; Schartel, B.; Russo, P.; Acierno, D. Polym Degrad Stab 2009, 94, 1245.
12. Braun, U.; Schartel, B. Macromol Mater Eng 2008, 293, 206.
13. Gallo, E.; Schartel, B.; Braun, U.; Russo, P.; Acierno, D. Polym Adv Technol 2011. doi: 10.1002/pat.1774.
14. Fu, S.-Y.; Feng, X. Q.; Lauke, B.; Mai, Y. W. Compos B 2008, 39, 933.
15. Casu, A.; Camino, G.; Giorgi, M. D.; Flath, D.; Laudi, A.; Morone, V. Fire Mater 1998, 22, 7.
16. Levchik, G. F.; Levchik, S. V.; Camino, G.; Weil, E. D. In Fire Retardancy of Polymers. The Use of Intumescence; Le Bras, M., Camino, G., Bourbigot, S., Delobel, R., Eds.; The Royal Society of Chemistry: London, U.K., 1998.
17. Jang, S. H.; Kim, Y. H.; Lim, S.; Choi, G. D.; Kim, S. H.; Kim, W. N. J Appl Polym Sci 2010, 116, 3005.